CONTACTLESS MEASUREMENT OF HEART SOUNDS AND HEART RATE WITH LASER DOPPLER VIBROMETRY

Kristian Kroschel[1], *Armin Luik*[2], *Jürgen Metzler*[3]

[1]*Karlsruhe Institute of Technology (KIT),* [2] *Klinikum Karlsruhe,* [3]*Fraunhofer Institute IOSB*
kristian.kroschel@kit.edu

Abstract: Currently heart sounds are picked up by a stethoscope from the thorax. In case of preterm infants and burnt clients a contactless method is preferred which might be based on laser Doppler vibrometer signals.

The raw vibrometer signal is sampled with the sampling frequency $f_s = 480$ Hz so that the usable upper frequency is $f_u = 240$ Hz. The mean of the vibrometer signal is suppressed. The heart sounds are extracted with a linear-phase band-pass filter with the passband 15 Hz $\leq f \leq$ 200 Hz. In the filtered signal the two heart sounds S_1 and S_2 of an adult client without any disease are visible and after transformation also audible.

Parallel to the vibrometer signal the electrocardiogram or ECG is monitored. After synchronisation of the filtered vibrometer signal with the ECG the coincedence of the S_1 sound with the R-spike of the ECG is visible. The same applies for the S_2 sound at the end of the T-wave.

The synchronism between the ECG and the heart sounds can be exploited to calculate the heart rate. First, the vibrometer signal is down sampled and filtered to extract the sound signal. The sound signal is rectified, filtered with a linear-phase band-pass filter with the passband adapted to the frequency range of the heart rate. Finally the heart rate extracted from the ECG and the vibrometer signal are compared to each other.

1 Introduction

The blood streams in the heart from the atria to the ventricles [3]. To avoid that the blood streams back when the heart chambers contract, valves are closed. The streaming blood and the closing and opening of the valves generate the heart sounds S_1 through S_4. Only the first two sounds are audible in case of adult clients without a disease. The other two sounds are audible only in case of diseases or with younger clients.

The standard method used to make the heart sounds audible is by a stethoscope which is pressed on the surface of the thorax. The standard location for this measurement is the third intercostal space or ICS, i.e. the space between the third and fourth ribs, about two fingers left of the breastbone. This is the so-called Erb point [8]. Clients with a sensitive skin like premature infants or burnt clients require a contactless method. Examples of these are the exploitation of a laser Doppler vibrometer signal [1], [2] or a radar signal [9]. The structure borne sounds of the blood flow and the operation of the valves propagate to the surface of the skin where the movement can be measured by the vibrometer. An infrared laser with the wavelength $\lambda = 1550$ nm is used because it is eye-friendly and commonly used in telecommunication applications

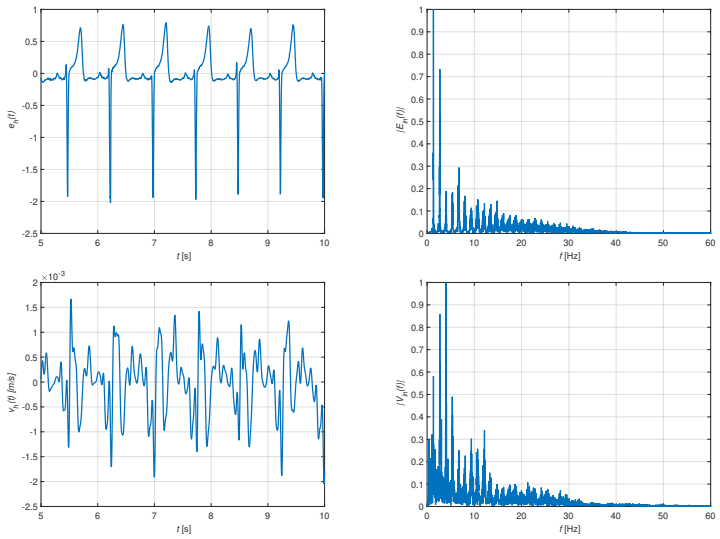

Figure 1 – ECG: time domain signal (top left), magnitude of the spectrum (top right). Vibrometer: time domain signal (bottom left), magnitude of the spectrum (bottom right).

which makes them cheap. To find an appropriate measuring point, a camera is used to direct a pan-tilt unit carrying the vibrometer to focus on the desired location.

Since the heart sounds are synchronised with the operation of the heart, the elctrocardiogram or ECG is picked up in parallel. The sound S_1 is linked with the R-peak [8], the largest peak of ECG, and the sound S_2 occurs at the end of the T-wave, the last wave at the end of the heart beat cycle. An example of the ECG and the vibrometer signal are shown in Figure 1. The sampling frequency is $f_s = 480$ Hz so that the spectra up to $f = 240$ Hz, the Nyquist frequency, could have been displayed. Since above $f = 60$ Hz is not much signal energy found, the spectra are shown only up to this frequency.

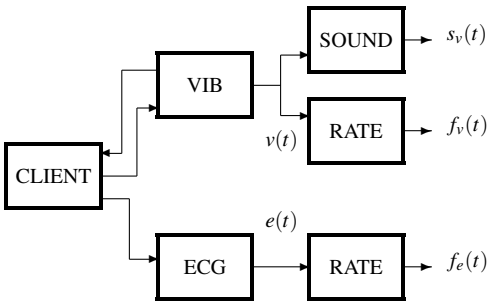

Figure 2 – Signal processing to extract the heart sounds and heart rate.

In the example in Figure 1 the R-peak is the negative maximum and the T-wave is visible at the end of the heart beat cycle. The periodicity of the heart beat is obvious as can be seen in the time domain of the ECG. For the vibrometer signal the periodicity is not that obvious in the time domain. The magnitudes of the spectra of both signals have been normalized with respect to their maximum and show a high similarity despite the fact that the ECG is an electrical signal and the vibrometer signal is the speed signal of the movement of the surface of the skin. Since both spectra consist of spectral lines their time domain equivalents are periodical. The fundamental frequency of the ECG is represented by the first spectral line at $f = 1.33$ Hz on the top in Figure 1 on the right. At the same frequency a spectral line is visible in the magnitude of the spectrum of the vibrometer signal. But in contrast to the ECG there are further spectral lines below this frequency which originate from breathing.

The heart sounds $s_v(t)$ are extracted from the vibrometer signal shown in Figure 1 by filtering

with a band-pass filter. The passband extends from $f = 15$ Hz up to $f = 200$ Hz and more. Since the heart sounds are synchronous with the heart rate $f_v(t)$, this parameter can be extracted from the heart sounds. This is shown in Figure 2. To evaluate the quality of the heart rate $f_v(t)$ calculated on the basis of the vibrometer signal, the heart rate $f_e(t)$ is derived from the electrocardiogram or ECG as shown in Figure 2. This heart rate serves as the reference.

Two devices pick up signals from the client (CLIENT): a vibrometer (VIB) and an ECG meter (ECG) which deliver at their output $e(t)$ and $v(t)$, respectively. The heart sound (SOUND) is extracted from the vibrometer signal $v(t)$ and the heart rate (RATE) from both, the ECG $e(t)$ and the vibrometer signal $v(t)$.

2 Extraction of the Heart Sounds

The heart sounds [4], [8] are found in the frequency band 15 Hz $\leq f \leq$ 150 Hz and above where heart murmurs and gallop rhythm occur. Therefore, a filter is used to extract these spectral components from the vibrometer signal $v(t)$. To avoid distortion, a linear-phase FIR filter with the transfer function [5]

$$H(z) = \frac{\sum_{i=0}^{n} b_i z^i}{z^n}, \quad b_i = b_{n-i},\ i = 1 \ldots n/2-1, n \text{ even},\ b_{n/2} \neq 0 \tag{1}$$

of order n with mirror-inverted coefficients b_i is used. There is not too much signal energy above $f =$ 60 Hz as can be seen in Figure 1 on the bottom right. Therefore the passband 15 Hz $\leq f \leq$ 150 Hz approximating the ideal filter chracteristic by the tolerance parameter $\delta = \pm 0.001$ is used. A good approximation of this characteristic is given by the order $n = 512$. The magnitude of the transfer function and the impulse response of this filter are shown in Figure 3.

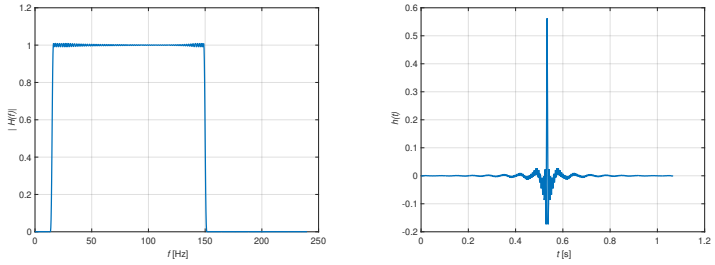

Figure 3 – Linear-phase sound filter: magnitude (left), impulse response (right).

The group delay of the filter is constant with $\tau_g = n/(2 \cdot f_s) = 0.53$ s. Since all the signals of interest are derived by filtering from the input signals, i.e., $e(t)$ and $v(t)$, and the filters are of the same order $n = 512$, these signals are synchronous to each other. The output of the filter and the magnitude of the spectrum are shown in Figure 4.

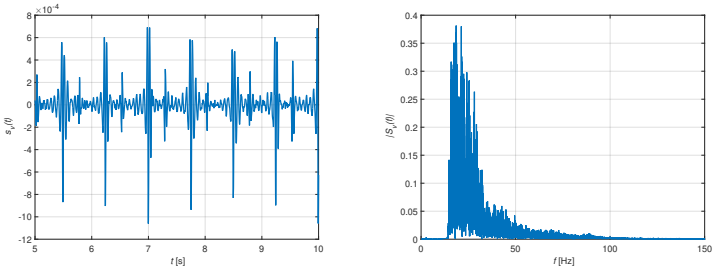

Figure 4 – The sound signal (left), the magnitude of its spectrum (right).

In each of the periods of the sound signal $s_v(t)$ the sounds S_1 and S_2 are visible and clearly distinguishable. From the magnitude of the spectrum follows that the upper cut-off frequency $f_u = 150$ Hz is large

enough to cover all spectral components of the heart sounds. The amplitude of S_1 is larger than that of S_2, both are not constant along the time axis. Also the shape of the sounds and their distance change with the running time. The magnitude of the spectrum decays rapidly so that above $f = 40$ Hz only a small percentage of energy is found. This opens the possibility to reduce the upper frequency if no details of the sound but only parameters like the heart rate are of interest.

The synchronism between the ECG with the heart sounds opens the possibility to compare the equivalence of the vibrometer signal $v(t)$ to the ECG $e(t)$. To suppress details of the vibrometer signal which are artifacts originating from movements of the client, breathing, coughing etc., the vibrometer signal is filtered by a linear-phase filter with the passband $0.75\ \text{Hz} \leq f \leq 20\ \text{Hz}$. This signal is called vibrocardiogram or VCG and is shown in Figure 5 together with the comparison of the VCG with the heart sound signal.

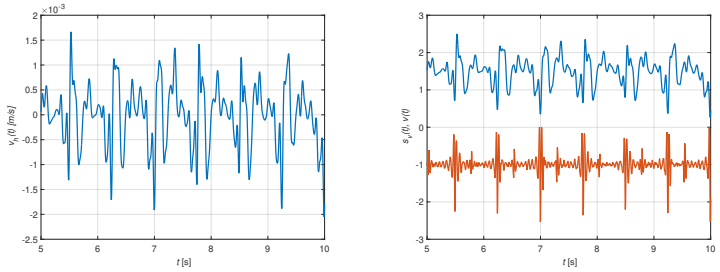

Figure 5 – VCG (left), comparison of the VCG with the sound signal (right).

A section of the sound signal covering roughly one period of the heart beat is depicted in Figure 6 together with a comparison of the ECG and the heart sounds. The ECG has been delayd by the group delay τ_g of the filter with which the vibrometer signal $v(t)$ has been filtered to extract the sound signal. Thus both signals are synchronous.

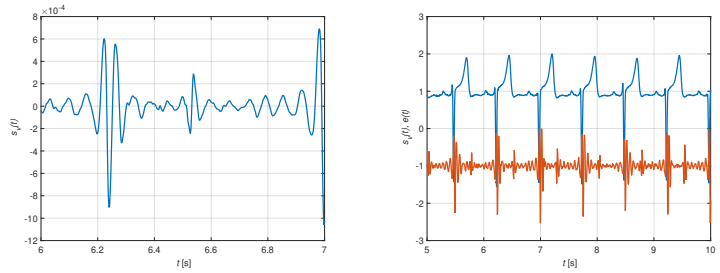

Figure 6 – Section of the sound signal (left), ECG and sound signal (right).

Paramters of the sounds S_1 and S_2 have been extracted from the sounds in Figure 6 on the left side. Their duration is $\Delta t_1 = 0.14$ s and $\Delta t_2 = 0.12$ s, respectively, and their frequency $f_1 = 22.8$ Hz and $f_2 = 28.4$ Hz, respectively. The sound S_1 is linked with the R-peak of the ECG which follows from the right part of Figure 6.

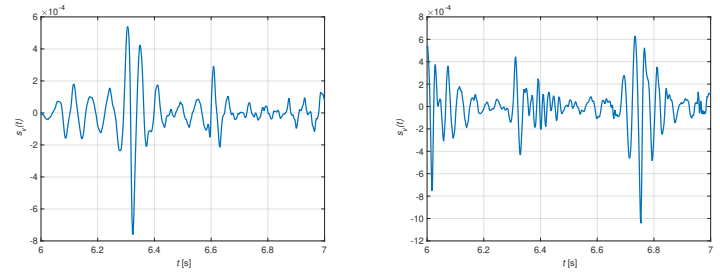

Figure 7 – Sections of the heart sounds. Picked up at the 2nd ICS left (left) and 4th ICS left (right).

The periodicity of the VCG is now clearly visible and by comparison of Figure 5 with Figure 6 follows

that the negative R-peak of the ECG complies with the negative maximum of the VCG. This opens the possibility to extract important parameters of the ECG like the PR-time from the VCG.

The extracted heart sounds depend on the point of measurement. This has already been investigated for the estimation of the heart rate [7] but applies also for the heart sounds. The heart sounds shown in Figure 6 have been picked up at the 3rd intercostal space (ICS) left of the breastbone. In Figure 7 the heart sounds picked up at the second and the fourth ICS left of the breastbone are shown.

The comparison of Figure 6 with Figure 7 shows significant differences. These are not only caused by the fact that these measurements have not been taken in parallel but serially. An other reason is that the distance to the valves depends on the location of measurement. The 2nd ICS left is closest to the pulmonary valve, the 3rd ICS left closest to the Erb point [8] which is the most appropriate location to measuere the heart sounds. The sounds do not only differ in their amplitude but also in their length and the relation of the amplitudes of the sounds S_1 and S_2 to each other. The differences are caused by the different transmission paths from their origin at the valves and the point of measurement. The attenuation and time delay of the transmission path for the structure borne sounds depend on the transmitting tissues.

3 Calculation of the Heart Rate from the Heart Sounds

The periodicity of the heart sounds is identical with the heart rate. Therefore the heart rate can be extracted from the heart sounds as is shown in Figure 8.

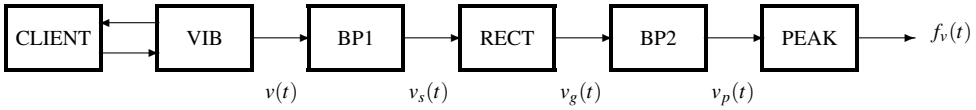

Figure 8 – Extracting the heart rate $f_v(t)$ from the heart sound $v_s(t)$.

Since now the details of the heart sounds are not important, the pass-band of the filter BP1 with which the heart sounds are extracted from the vibrometer signal $v(t)$ can be reduced. From Figure 4 follows that above $f = 40$ Hz the magnitude of the spectrum decays rapidly. Therefore the reduced passband 15 Hz $\leq f \leq$ 40 Hz is chosen. From this limitation results the magnitude of the spectrum $V_s(f)$ and the time domain signal $v_s(t)$ shown in Figure 9.

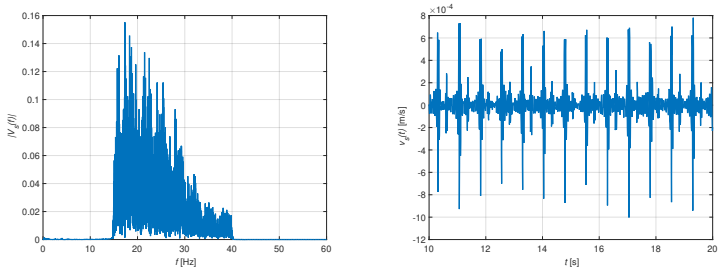

Figure 9 – Magnitude of the spectrum $V_s(f)$ with reduced bandwidth (left) and corresponding sound signal $v_s(t)$ (right).

The sound signal $v_s(t)$ shown in Figure 4 and Figure 9 are eqivalent to each other. They differ only in detail, but still the time domain representation of the sounds S_1 and S_2 is visible. For the calculation of the frequency, the peaks of the signal have to be localized. Since the peaks are not unique but might be split as can be seen in Figure 6 on the left side and are bipolar, preprocessing is required before the peaks are extracted. The first step is rectification in block RECT, so that a unipolar signal $v_g(t)$ is generated. Furthermore, it has to be taken into account that the heart rate of an adult without a disease is limited to 40 bpm $\leq f_h \leq$ 120 bpm with bpm for beats per minute. For the design of a filter, this corresponds with the pass-band 0.66 Hz $\leq f \leq$ 2 Hz of filter BP2. Again, a linear-phase filter of order $n = 512$ with

the same tolerance parameters as before will be used. The rectified vibrometer signal $v_g(t)$ filtered by a band-pass filter with passband 0.75 Hz $\leq f \leq$ 20 Hz and the rectified and filtered sound signal $v_p(t)$ are shown in Figure 10.

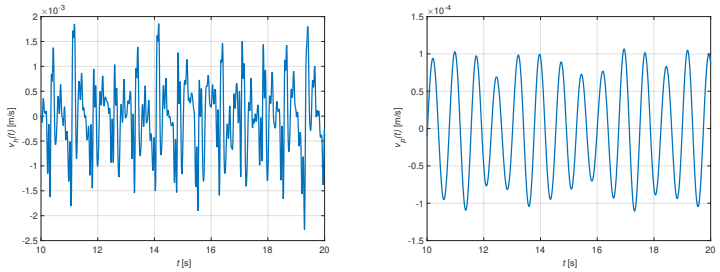

Figure 10 – VCG (left), rectified and filtered sound signal (right).

The correspondence of the peaks of the VCG and the rectified and filtered or preprocessed sound signal $v_p(t)$ is clearly visible. The advantage of the preprocessed vibrometer signal $v_p(t)$ is the uniqueness of the peaks. With a simple peak detector these peaks can be extracted unambiguously. If two consecutive maxima of $v_p(t)$ are found at t_i and t_{i-1}, respectively, then the heart rate at $t = t_i$ measured in bpm is given by

$$f_h(t) = \frac{60}{t_i - t_{i-1}} \; [bpm]. \tag{2}$$

In the previous section the heart sounds measured at three locations, the 2nd, 3rd and 4th ICS left of the breastbone have been compared to each other. The same is done here with the equivalent heart rates. In Figure 11 the heart rates measured at these locations are shown and the parameters μ and σ extracted from the ECG and the vibrometer signal for all three heart rates are compared to each other in Table 1.

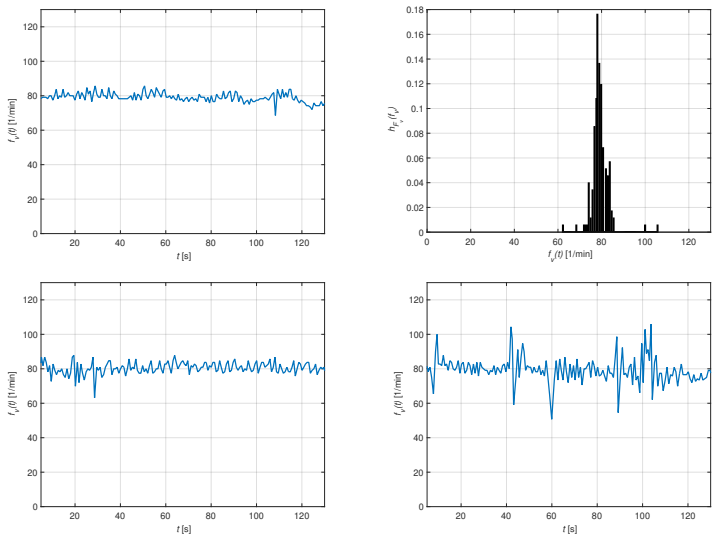

Figure 11 – Heart rate at the 3rd ICS left (top left) and histogram (top right). Heart rate at the 2nd ICS left (bottom left) and at the 4th ICS left (bottom right).

The heart rate is characterized by a clearly visible roughness which differes significantly at the three measuring points. As expected, the result from the Erb point depicted on the top is the most appropriate one. This is underlined by the mean μ and standard deviation σ summarized in Table 1.

To evaluate this result, the corresponding parameters extracted from the ECG are used. The ECG is characterized by unique sharp R-peaks which could be used to determine the time instances t_i in Equation 2. But to include the influence of the method to determine the peaks in the case of the sound signal, the ECG is rectified and filterd in the same way as was done with the sound signal. This approach is motivated by

ICS	μ_v	σ_v	μ_e	σ_e	*mse*
2nd, left	80.29	4.02	80.22	2.47	0.64
3rd, left	79.18	3.95	79.05	2.20	1.30
4th, left	79.56	7.95	79.43	3.86	2.11

Table 1 – Comparison of the heart rates at three measurement points. All figures given in bpm.

the fact that the R-peaks might be positive or negative depending on the pick-up of the ECG. The ECG and the rectified and filtered version are given in Figure 12 on the top. Extraction of the time instances t_i of the maxima and using them in Equation 2 delivers the heart rate which is shown together with the histogram in Figure 12 on the bottom.

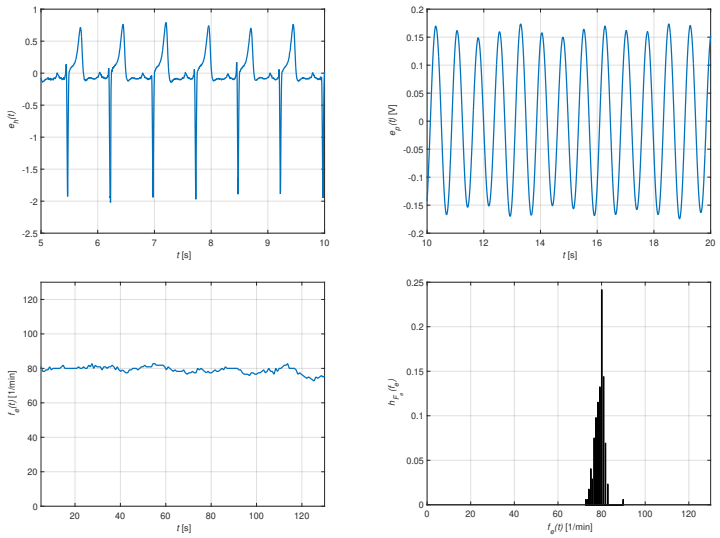

Figure 12 – Synchronized ECG (top left), rectified and filtered ECG (top right). Heart rate (bottom left) and histogram (bottom right).

The roughness of the heart rate $f_e(t)$ calculated from the ECG is lower compared to the heart rate $f_v(t)$ based on the sound signal as follows from the comparison of Figure 11 and Figure 12. This is underlined by the mean μ and standard deviation σ found in Table 1. Furthermore the mean square error *mse* between the heart rates $f_e(t)$ and $f_v(t)$ is calculated. The *mse* is smallest for the 2nd ICR left but the standard deviation σ_v is smallest for the 3rd ICS left which is more important.

For the interpretation of the three results it has to be taken into account that the measurements have been picked up at three time instances following one after the other by $\Delta t = 240$ s. Therefore the heart rate extracted from the ECG differs in all three cases slightly by 0.8 bpm and 1.2 bpm, respectively. In general, the standard deviation is less for the ECG based heart rate compared to the result gained from the vibrometer signal $v(t)$. The result from the 4th ICS left is the less reliable whereas the results from the 2nd and 3rd ICS left are quite close together. But the differences between those based on the ECG and the sound signal are low in general.

4 Summary and Outlook

It has been shown that the heart sounds S_1 and S_2 can be extracted from the vibrometer signal by appropriate filtering. Since the sound S_1 is aligned with the R-peak of the ECG, the equvalent to the R-peak in the VCG can be found. This might be the entry point to extract other prominent points like P so that descriptive values like the length of the PQ-wave can be identified in the VCG.

There are various possibilities [6] to estimate the heart rate on the basis of the vibrometer signal. Most of them require averaging like the methods based on the fast Fourier transform or FFT and the autocorrela-

tion function. Because of the noise of the vibrometer signal originating from the movement of the client, his utterance or coughing, these influences are reduced by averaging. Averaging obstructs the calculation of the instantaneous heart rate. The method for the calculation of the heart rate from the heart sound does not require averaging for the calculation of the heart rate so that the instantaneous frequency is available. It has not yet been investigated how the movements of the client or uttering and coughing influence the calculation of the heart rate on the basis of the heart sound.

The contact-free measurement of the heart sound has shown a great potential in an initial pilot test. It was possible to make the heart sounds audible and the medical interpretation seems to be realistic. Comparative measurements with well-established methods based on the stethoscope, e.g., have to prove that diseases of the heart walves can be reliably detected.

Acknowledgement

The investigations presented in this paper have been supported by a grant from the German Ministry of Education and Research under the contract 13N13725 in the framework of the the project Tricorder. The vibrometer signals have been picked up in the Klinikum Karlsruhe and the vibrometer was a contribution of the company Polytec from Waldbronn, a partner within this project. The authors thank for all the help, discussions and advice from the staff of our partners.

References

[1] BAI, J., SILESHI, G., NORDEHN, G., BURNS, S., WITTERS, L.: Development of laser-based heart detection systems. Journal of Biological Science and Engineering 5, 34-37, 2012

[2] DE MELIS, M., MORBIDUCCI, U., SCALISE, L.: Identification of cardiac events by Optical Vibrometry: comparison with Phonocardiography. In: Proc. 29th Annual Conference of the IEEE EMBS, pp. 2956-2959, 2007

[3] HALL, J.E.: Guyton and Hall Textbook on Medical Physiology. Elsevier ISBN 3-11-0157144-4, 2005

[4] HOTH, M., WISCHEMEYER, E.: Herztöne und Herzgeräusche. In: Behrends, J.C. (ed.) Duale Reihe Physiologie. Georg Thieme Verlag ISBN 978-3-13138-411-9, 2010

[5] KAMMEYER, K.-D., KROSCHEL, K.: Digitale Signalverarbeitung. Springer-Vieweg, Wiesbaden 2018

[6] KROSCHEL, K., LUIK, A.: Laser-based remote measurement of vital parameters of the heart. Proc of SPIE vol. 10680, Strasbourg 2018, pp. 1068000-2 - 1068000-8, 2018

[7] KROSCHEL, K., METZLER, J.: Lokalisation des optimalen Messorts zur berührungslosen Bestimmung von Puls- und Atemfrequenzen. 28. Konferenz Elektronische Sprachsignalverarbeitung, pp. 300-387, Saarbrücken 2017

[8] VON WESTPHALEN, Graf G., ANTWERPES, F., STEIGENBERGER, P., FINK, B.: Herzton. https://flexicon.doccheck.com/de/Herzton. Cited 19 November 2019

[9] WILL, C., SHI, K., SCHELLENBERGER, S., STEIGLEDER, T., MICHLER, F., FUCHS, J., WEIGEL, R., OSTGATHE, C., KOEPLIN, A.: Radar Based Heart Sound Detection. Scientific Reports 8, doi:10.1038/s41598-018-29984-5, 2018